forests

MDPI

Article

Development of a Climate-Sensitive Structural Stand Density Management Model for Red Pine

Peter F. Newton

Canadian Wood Fibre Centre, Canadian Forest Service, Natural Resources Canada, Sault Ste. Marie, ON P6A 2E5, Canada; peter.newton@nrcan-rncan.gc.ca; Tel.: +1-705-541-5615; Fax: +1-705-541-5700

Abstract: The primary objective of this study was to develop a climate-sensitive modular-based structural stand density management model (SSDMM) for red pine (*Pinus resinosa* Aiton) plantations situated within the western Great Lakes—St. Lawrence and south-central Boreal Forest Regions of Canada. For a given climate change scenario (e.g., representative concentration pathway (RCP)), geographic location (longitude and latitude), site quality (site index) and crop plan (e.g., initial espacement density and subsequent thinning treatments), the resultant hierarchical-based SSDMM consisting of six integrated modules, enabled the prediction of a multitude of management-relevant performance metrics over rotational lengths out to the year 2100. These metrics included productivity measures (e.g., mean annual volume, biomass and carbon increments), volumetric yield estimates (e.g., total and merchantable volumes), pole and log product distributions (e.g., number and size distribution of pulp and saw logs, and utility poles), biomass production and carbon sequestration outcomes (e.g., oven-dried masses of above-ground components and associated carbon mass equivalents), recoverable end-product volumes and associated monetary values (e.g., volumes and economic worth estimates of recovered chip and dimensional lumber products extractable via stud and randomized length mill processing protocols), and crop tree fibre attributes reflective of end-product potential (e.g., wood density, microfibril angle, and modulus of elasticity). The core modules responsible for quantifying stand dynamics and structural change were developed using 491 tree-list measurements and 146 stand-level summaries obtained from 98 remeasured permanent sample plots situated within 21 geographically separated plantation-based initial spacing and thinning experiments distributed throughout southern and north-central Ontario. Computationally, the red pine SSDMM and associated algorithmic analogue (1) produced mathematically compatible stem and end-product volume estimates, (2) accounted for density-dependent as well as density-independent mortality losses, response delay following thinning and genetic worth effects, (3) enabled end-users to specify merchantability standards (log and pole dimensions), product degrade factors and cost profiles, and (4) addressed climate change impacts on rotational yield outcomes by geo-referencing RCP-specific effects on stand dynamical processes via the deployment of a climate-driven biophysical site-based height-age model. In summary, the provision of the red pine SSDMM and its unique ability to account for locale-specific climate change effects on crop planning forecasts inclusive of utility pole production, should be of consequential utility as the complexities of silvicultural decision-making intensify during the Anthropocene.

Keywords: stand-level distance-independent average-tree and size-distribution yield model; representative concentration pathway; utility pole production; computation pathway; decision-support system; algorithmic analogue

Citation: Newton, P.F. Development of a Climate-Sensitive Structural Stand Density Management Model for Red Pine. *Forests* **2022**, *13*, 1010. https://doi.org/10.3390/f13071010

Received: 26 May 2022
Accepted: 17 June 2022
Published: 27 June 2022

1. Introduction

Red pine (*Pinus resinosa* Aiton) is an intensely managed and fire-adapted species that occupies a wide range of sandy-textured sites throughout the Great Lakes Region of North America. For over a century, red pine has been one of the primary species used

in reforestation and afforestation efforts, particularly throughout the western portion of the Great Lakes—St. Lawrence Forest Region [1], southern sections of the Boreal Forest Region [1] and Northern Lakes and Forests Ecoregion spanning the northern sections of the western Lake States [2]. Plantation-based productivity comparisons with other conifers have revealed that intensely managed red pine plantations can at least double rotational volumetric yields and produce a broader array of high-value end-products, including utility poles, compared to similarly treated black spruce (*Picea mariana* (Mill) B.S.P.) and white spruce (*Picea glauca* (Moench) Voss) plantations growing on equivalent site qualities at the same locale (e.g., 2- and 3-fold increases in volumetric yield, respectively; [3]). Conditional on the availability of acceptable sites in terms of local biotic, edaphic and climatic conditions, the range of red pine has also been forecasted to shift in a north-eastern direction throughout the central portion of the Canadian Boreal Forest Region under climate change [4]. Furthermore, observational reports have indicated a possible climate-induced westward expansion throughout the northern portion of the continental USA (e.g., [5]). However, arriving at a general consensus on climate-induced migration patterns remains elusive, given the observed sensitivity of the species to localized variability in temperature and moisture extremes (e.g., [6,7]).

Apart from the possible changes in the species range arising from climate change, practicing optimal crop planning could yield benefits in terms of enhancing carbon sequestration and retainment rates. More precisely, experimental evidence from the Lake States indicate that intermediate stand-tending thinning treatments within red pine plantations could enhance their climatic resilience via increases in residual crop tree vigour arising from a reduction in competition stress [8]. Regulating site occupancy through density management could also yield increases in photosynthetic-induced CO_2 uptake arising from accelerated rates of tree growth, decreases in decomposition-induced CO_2 release arising from reduced rates of density-dependent mortality (e.g., lower rates of abiotic mass generation), and increases in long-term sequestrated CO_2 retainment arising from the increased production of long-lived solid-wood end-products (e.g., dimensional lumber and utility poles). The latter may also have beneficial consequences in terms of material substitution (e.g., replacement of fossil-derived carbon-intensive building products; [9]).

Climate change environment-based growth determinates, such as localized precipitation rates and mean temperatures (bioclimatic variables), directly affect dominant height developmental patterns in red pine [7]. Consequently, the rates of stand development and ultimately rotational productivity will vary by the degree of future climate change severity. More precisely, within the context of the representative concentration pathway (RCP) framework established by the Intergovernmental Panel on Climate Change (IPCC [10]), the magnitude of climate change effects on red pine productivity is expected to vary by RCP scenario (e.g., RCP8.5 > RCP4.5 > RCP2.6) and temporally within a given RCP, by commitment period (e.g., 2010–2040 < 2041–2070 < 2071–2100) (sensu [7]). Thus given the increased interest in the utility of red pine within the context of climate change adaption and mitigation efforts (e.g., natural climate solutions such as afforestation and reforestation; e.g., [11]) and acknowledgment that red pine productivity will vary by RCP and commitment period, the provision of a crop planning tool such as a climate-sensitive structural stand density management model (SSDMM) would be a welcome development for red pine foresters, managers and silviculturists (sensu [12]).

Briefly, the SSDMM is a variable–density yield and wood quality size-distribution model, which could be classified as a hybrid average tree and stand-level distance-independent size-distribution model, according to the nomenclature advanced by Porté and Bartelink [13]. Historically, the analytical lineage of this modelling approach arose some 60 years ago via the introduction of stand density management diagrams (SDMDs; [14]). Specifically, their developmental pathway has been characterized by three sequential phases during which model complexity, scope and application diversity has systematically increased [14]: static SDMDs (1962–1992+) → dynamic SDMDs (1993–2008+) → structural SDMDs (2009–2021+). Furthermore, the recently introduced climate-sensitive SSDMM variants that have been

developed for a number of boreal coniferous stand-types, have the potential to extend the utility of SSDMMs in crop planning decision-making during the Anthropocene (sensu [14,15]).

Consequently, as part of a larger inter-agency participatory-based effort (sensu [16]) to develop a suite of comprehensive decision-support tools for operational deployment in managing commercially important coniferous species (sensu [17]), the objective of this study was to develop a climate-sensitive modular-based SSDMM and associated software analogue for red pine plantations. Analytically, this consisted of employing the generalized parameterization framework introduced in the development of the SSDMM for jack pine [18] in combination with some of the more recently introduced innovations advanced within this modelling domain. More precisely, these advancements included: (1) ensuring mathematical compatibility in volumetric predictions (e.g., constraining the cumulative chip and lumber volume estimate to be equivalent to the merchantable volume estimate in cases were such cumulative volumes exceeded this estimate [19]); (2) accounting for density-independent mortality from extraneous factors such as insects and disease through the use of an end-user-specified operational adjustment factor [19]; (3) integrating a crown occupancy algorithm to account for the temporal response delay effect that arises when trees within recently thinned stands are adjusting to their newly allocated space and site resources [19]; (4) accounting for genetic worth and thinning release effects on growth and stand dynamical processes through a functional adjustment to the site-based height-age equation (e.g., [20] and [21], respectively); (5) incorporating a geographical-referencing biophysical height-age function to account for climate-induced site productivity changes and associated effects on stand dynamical processes over three continuous 30-year commitment periods [7]; and (6) integrating a suite of end-product-based fibre attribute models for predicting wood quality determinates at rotation [22]. The scope of this presentation deals exclusively with the (1) model structure and associated module-specific functional specifications and parameterization analytics inclusive of statistical performance assessments, and (2) computational pathways within and among modules. Extensive provincial-wide exemplifications of the model's utility in crop planning decision-making under various climate change scenarios, along with an assessment of the model's overall predictive ability, are to be reported concurrently within a companion contribution [23].

2. Materials and Methods

2.1. Data Sets, Preliminary Calculations, and Descriptive Statistics

Subsequent to conducting a comprehensive data quality review and verification procedure of the accessible sample plot records within the Province of Ontario, 491 tree-list measurements and 146 stand-level summaries were obtained from 98 permanent and experimental sample plots situated within 21 geographically-separated plantation-based density management experiments or monitoring plot clusters. These plots were within plantations subjected to a range of initial spacing (IS) and thinning treatments and were periodically remeasured from 3 to 10 times over relatively long observational periods (e.g., multi-decadal; Table A1 (Appendix A)). Nineteen experiments or monitoring plot clusters were located within Forest Sections L.1, L.2, L.4c and L.4d of the Great Lakes—St. Lawrence Forest Region [1], which falls within the province's southern administrative region. These are referenced by a geographic-based location denotation that was previously established either by the Canadian Forest Service (CFS) or the Ontario Ministry of Natural Resources and Forestry (OMNRF): Petawawa National Forestry Institute (AECL (Atomic Energy of Canada Limited) spacing trial); Ballycroy (north-east of Lake Simcoe); Barr North (north-east of Lake Simcoe); Charlebois (Port Elgin area); Durham UX Main (Uxbridge area); Durham UX West (Uxbridge area); Flinton (north-west of Kingston); Larose (north-east of Ottawa); Limerick South (north of Belleville); McArthur (south of Honey Harbor, Georgian Bay); Orr Lake Hamilton; Orr Lake Main; Orr Lake Stoney; Orrock North East (Simcoe Country Forest; north of Toronto); Orrock South (Simcoe Country Forest; north of Toronto); Rockland (east of Ottawa); Sauble Beach (Port Elgin area); Slessor (North Bay area); and Vivian (north of Toronto). The remaining 2 experimental installations were located within

the central administrative region of Ontario: Kirkwood (north of Thessalon) and Thunder Bay (western area), which fall within the Forest Section L.10 of the Great Lakes—St. Lawrence Forest Region [1] and Forest Section B.9 of the Boreal Forest Region [1], respectively. Silviculturally, 20 plots were subjected solely to IS treatments, whereas the remaining 78 plots were subjected to either a single thinning treatment or a multiple sequential series of thinning treatments (maximum of 7; Table A1).

At each temporal measurement, the collected tree-list data consisted of an identification label (number), species, biotic/abiotic status and diameter at breast-height (1.3 m; D (cm)) for each tree that had attained a minimum breast-height diameter of 2.54 cm. In total, 491 temporal-specific plot-based tree-list remeasurements were utilized, from which mean tree and stand-level mensurational variables were subsequently generated along with diameter distribution metrics. More precisely, the preliminary computations required to generate the mensurational variates for the 491 plot remeasurements involved the following: (1) deploying an existing height-diameter equation [24], individual tree heights (H (m)) were generated for each biotic tree; (2) given (1), the resultant height distribution was generated and the mean dominant height for each temporal-specific plot measurement calculated (i.e., mean height of all trees within the upper height quintile; H_d (m)); (3) given (2), deploying the H_d estimate along with establishment age information, a site index value (mean dominant height at a breast-height age of 50 years; [7]; S_I (m)) was generated for each temporal-specific plot measurement from which a plot-specific mean was calculated and assigned; (4) total plot-based basal area and density were calculated and scaled to the per hectare level using the plot area information, yielding stand-level basal area (G (m^2/ha) and total density (N (stems/ha)) estimates, respectively, for each temporal-specific plot measurement; (5) total volume (V_t; m^3/ha) was calculated as the scaled sum of the individual tree total volumes as determined from the D and H measurements in combination with a regional-wide standardized total volume equation parameterized for red pine [25]; and (6) merchantable volume (V_m; m^3/ha) was calculated as the scaled sum of the individual tree merchantable volumes for all trees greater than 9 cm in D as calculated using a regional-wide standardized merchantable volume equation developed for red pine [25] (i.e., utilizing the D and H measurements, individual tree total volume estimate, merchantability limit specifications (0.1524 m stump-height and a 7.62 cm merchantable top diameter (inside bark)) and plot area information, individual-tree and stand-level merchantable stem volume estimates were computed). This computational sequence yielded the following mensurational metrics for each of the 491 temporal-specific plot measurements: mean stand and breast-height age (A and A_{bh}, respectively; yr), H_d, mean S_I, quadratic mean diameter (D_q; cm), G, V_t, V_m and N. Although 146 of the temporal-specific plot remeasurements lacked the tree-list data required for generating these metrics, mean tree and stand-level mensurational variable estimates were nevertheless extracted from previous documented analyses and utilized accordingly.

Overall, the plots ranged in age from 10 to 87 years and in dominant height from 4.1 m to 33.3 m (Table A1), thus covering a wide spectrum of this species stand developmental phases: e.g., stand initiation → open-grown and pre-crown closure → stem exclusion and post-crown closure (self-thinning) → chronological maturity. Furthermore, the plots were situated on a range of site qualities representative of the species' commercial productivity within the study region (Table A1): site indices (mean dominant height at a breast-height age of 50 yr; [7]) ranging from 16.1 m (lower productivity quartile) to 27.1 m (upper productivity quartile) with an overall mean value of 22.8 m. The range of density management treatments were also reflective diverse silvicultural intensities (basic to intense) which generated a wide array of site occupancy and stocking conditions (e.g., absolute plantation densities varying from 300 to 5600 stems/ha (Table A1)). Refer to Table A1 for complete variable-specific descriptive statistics for all 637 temporal-specific plot measurements utilized: e.g., sample-site-specific statistics for age, site index, quadratic mean diameter, mean dominant height, basal area, merchantable and total volumes, and density, along with information

pertaining to plot size, measurement sequence, and thinning treatment(s), for each of the 21 locales.

2.2. Modular-Specific Development of the Red Pine SSDMM

Apart from the novel introduction of a biophysical site index model to account for climate change effects and enable spatial-based red pine crop planning, and changes to the SSDMM model structure to accommodate the prediction of a new end-product group (utility poles) and an array of end-product Silviscan-based fibre determinates, the analytics deployed largely followed those previously established within this modelling domain (sensu [26–29]). Specifically, the hierarchical-based red pine SSDMM consisted of six sequentially linked prediction modules: Module A—Dynamic SDMD; Module B—Diameter and Height Recovery; Module C—Taper Analysis and Pole, Log and Stem Volume Estimation; Module D—Biomass and Carbon Estimation; Module E—Mill-Specific Product Recovery and Value Estimation; and Module F—Fibre Attribute Estimation. A schematic illustration of the structure of the SSDMM, including the interrelationships and sequential flow of computations among the individual modules, along with generic input requirements and resultant output metrics, is provided in Figure 1.

Analytically, Module A involved the development of a climate-sensitive red pine dynamic SDMD via the parameterization and integration of a broad array of static and dynamic yield–density relationships employing the traditional SDMD modelling framework along with the introduction of a biophysical site-specific height-age function to account for climate change effects and a set of sub-models to address genetic worth and thinning response effects (sensu [15,20,21,26]). Module B consisted of the development of a (1) Weibull-based parameter prediction equation system (PPES) for diameter distribution recovery, and (2) composite height-diameter prediction equation for diameter-class-specific height estimation. Module C deployed a dimensional compatible taper equation parameterized for red pine by Sharma [27] to predict stem product yields (number of pulp and saw logs, and utility poles) and stem volumes at the individual tree, diameter class and stand levels. Module D entailed the employment of allometric-based biomass equations developed for red pine by Lambert et al. [28] to estimate above-ground total and component (periderm, stem, branch and foliage) biomasses and associated carbon-based equivalent masses, at the individual tree, diameter class and stand levels. Module E utilized jack pine sawmill-specific (stud and randomized length) product and value equations as surrogate prediction functions to generate chip and lumber volume estimates and associated monetary values at the individual tree, diameter class and stand levels. Note, fiscal worth estimates for recovered utility poles were computationally added to the chip and lumber monetary values in order to generate stand-level revenue estimates (i.e., cumulative chip and lumber inflation-adjusted fiscal worth estimates for the log (10–32 cm) and pole (34+ cm) producing diameter classes). Module F encompassed the employment of a suite of previously developed Silviscan-based attribute prediction models for red pine in order to generate estimates of the principal fibre determinates underlying end-product potential (i.e., wood density, microfibril angle, modulus of elasticity, fibre coarseness, tracheid wall thickness, tracheid radial diameter, tracheid tangential diameter and specific surface area; [29]).

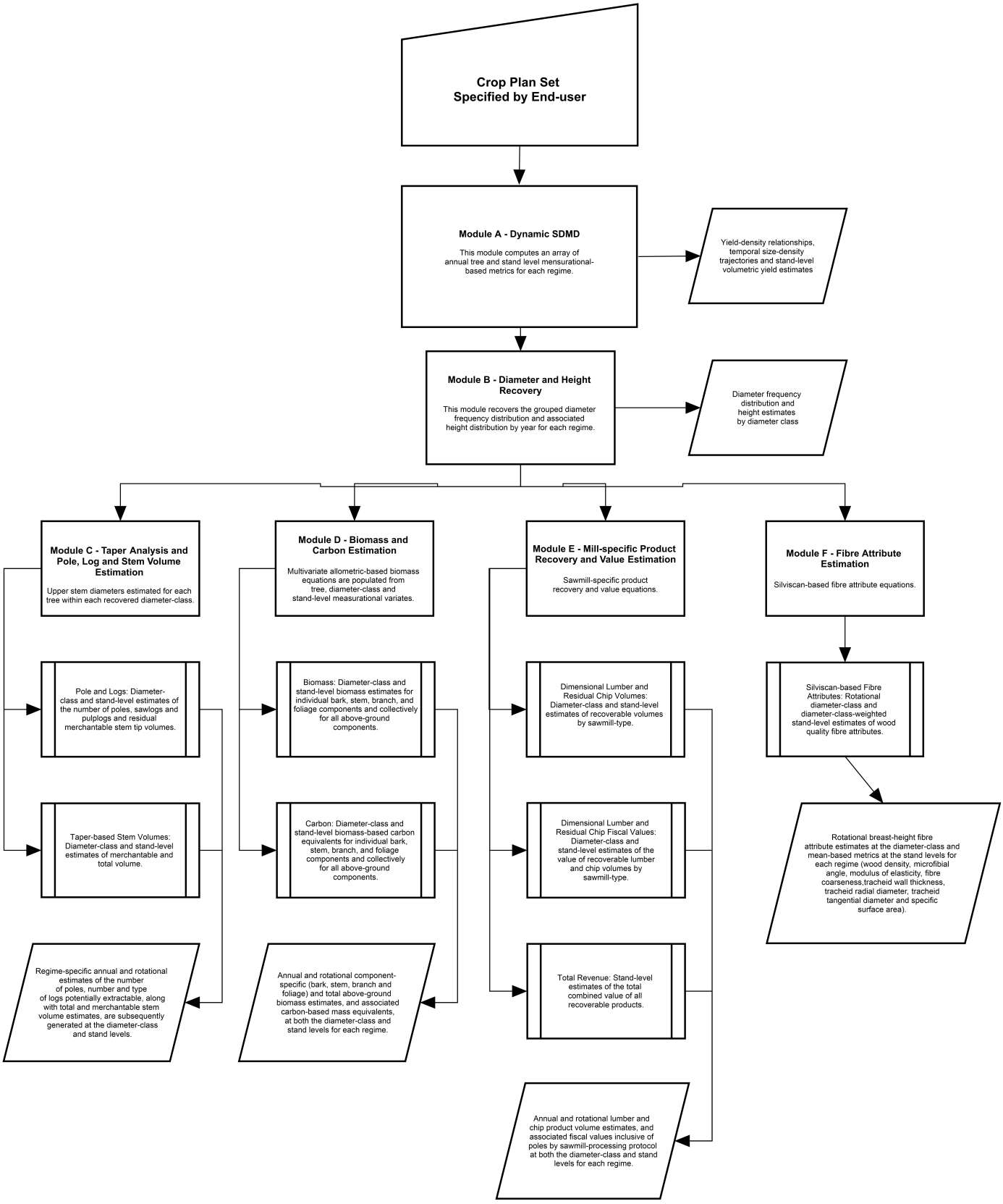

Figure 1. Schematic illustration of the modular-based SSDMM for red pine (sensu Figure 1 in Newton [17]): hierarchical structure and computational pathway.

The model requires input in terms of the following crop plan specifications: site index, locale, and a triple set of density management regimes specifying their (1) establishment

density and rotation age, (2) climate change scenario inclusive of associated commitment-period-specific temperature and precipitation values, (3) time, type, growth response model, intensity and costs of thinning treatments when applicable, (4) genetic worth effects, selection age and associated growth response model type when applicable, (5) site preparation, establishment and rotational harvesting costs, and (6) inflation and discount rates, calendar year of simulation, operability targets, merchantability specifications for stem volumes, saw and pulp logs, and poles, fiscal worth estimate for utility poles, and the operational adjustment factor. Given this input, the computation flow follows a hierarchical pathway, as illustrated in Figure 1.

Presentation-wise, given that several of the required relationships involved extensive analytics in terms of parameterization and evaluation (e.g., yield–density and asymptotic size–density relationships, Weibull-based PPES, and composite height-diameter functions) and hence represented new contributions, explicit analytical details are provided. Specifically, as documented within the Supplementary Materials file SM-S1.PDF. Additionally, in cases where the prerequisite relationships could not be developed given data limitations, literature-derived functions were deployed. These included the biophysical site index, taper, biomass and Silviscan-based fibre equations developed by Sharma and Parton [7], Sharma [27], Lambert et al. [28] and Newton [29], respectively. Furthermore, in situations where the required relationships could not be extracted from either the available data or literature-based sources, jack pine surrogate equation equivalents were deployed (i.e., product volume and value relationships developed by Newton [18]). Considering that these surrogate equations utilize stem diameter and height as independent tree-level predictor variables, and fiscal values for chip and lumber products are generally similar, the jack pine based estimates were not expected to be consequentially dissimilar. Furthermore, in order to provide a comprehensive description of the hierarchical module-based structure and the iterative nature of the model building approach utilized, a complete account of the deployed analytics and associated results is presented in a sequential fashion. For newly developed relationships, information pertaining to the overall approach and data sets utilized, statistical analyses, and resultant parameter estimates obtained, along with applicable goodness-of-fit and predictive performance measures, are explicitly included. For relationships extracted from the literature, the appropriate reference is provided along with the functional expression inclusive of the reported parameter estimate values. A detailed description of the computational sequence deployed within the resultant SSDMM along with pertinent schematic illustrations for each module, all cross-referenced with the parameterized functions utilized, is also provided. Specifically, as documented within the Supplementary Materials file SM-S2.PDF.

The computational sequence was then encapsulated within a deployable algorithmic analogue, ultimately yielding the climate-sensitive red pine crop planning decision-support tool. This comprehensive and transparent account of the modelling approach and associated analytics inclusive of the computational pathways deployed, is provided in order to facilitate model replication, allow for future model modification, and enable an in-depth assessment of the underlying relationships and associated assumptions utilized.

3. Results and Discussion

3.1. The Climate-Sensitive Modular-Based SSDMM for Red Pine

Firstly, the dynamic stand density management diagram was developed via the determination and subsequent integration of the following relationships: (1) asymptotic mean volume–density relationship and associated relative density index (P_r) function (Equation (S1) and Equation (S2), respectively) and resultant P_r isolines (Equation (S3)); (2) yield–density relationships and associated isolines for quadratic mean diameter (Equation (S4) and Equation (S5), respectively), mean dominant height (Equation (S6) and Equation (S7), respectively), and mean live crown ratio (Equation (S8) and Equation (S9), respectively); (3) mean volume–density relationships at the time of initial crown closure (Equation (S10)) and those delineating the zone of optimal volumetric production (P_r = 0.35 (lower boundary) and P_r = 0.50

(upper boundary)); and (4) survivorship function for predicting post-crown-closure size–density trajectories (Equation (S11)). The graphical representation of the dynamic SDMD was constructed by superimposing the following relationships on a bivariate logarithmic graph with mean volume on the ordinate axis and stand density on the abscissa: (1) asymptotic size–density relationship (self-thinning rule; Equation (S1)); (2) isolines for relative density index, quadratic mean diameter, mean dominant height, and mean live crown ratio (Equation (S3), Equation (S5), Equation (S7) and Equation (S9), respectively); (3) crown closure line (Equation (S10)); (4) lower and upper P_r isolines delineating the conceptual-based optimal density management window ($0.35 \leq P_r \leq 0.50$); and (5) expected size–density trajectories for a given crop plan as predicted by the net density change function (Equation (S11)) in association with the site-based height-age function (Equation (1)) and the operational adjustment factor which is used to account for annual density-independent mortality losses throughout the rotation.

Similar to the methodology previously used in the development of the climate-sensitive SSDMM variants for jack pine and black spruce stand-types ([15,17]), the SSDMM structure was modified by incorporating the biophysical site-based height-age model developed for red pine by Sharma and Parton ([7]; Equation (1)). This rate modifier approach attempts to reflect localized climate change effects on stand dynamical processes using the site-based mean dominant height-age function. Conceptually, it is similar to the response modelling methodology used to adjust various tree and stand growth and yield models in order to account for silvicultural treatment effects (sensu [30]): e.g., modifying the existing site productivity function that governs the temporal development of the size–density trajectory via the introduction of climate-sensitive rate parameter modifiers (precipitation and temperature variables). As a consequence, two variants of the red pine SSDMM were generated depending on which site-specific height-age model is utilized: (1) climatic-insensitive variant when deploying Equation (1a); and (2) climate-sensitive variant when deploying Equation (1b).

$$H_d = 43.7309 / \left(1 - \left(1 - \frac{43.7309}{S_I}\right)\left(\frac{50}{A_{bh} - 0.5}\right)^{1.2000}\right) \quad (1a)$$

$$H_d = 26.2695 + 0.03355P_{g(jkl)} / \left(1 - \left(1 - \frac{26.2695 + 0.03355P_{g(jkl)}}{S_I}\right)\left(\frac{50}{A_{bh} - 0.5}\right)^{2.3244 - 0.8297T_{g(jkl)}}\right) \quad (1b)$$

where H_d is the predicted mean dominant height (m) at a given breast-height age (A_{bh} (yr)) for a specified site quality as quantified by site index (S_I (m); i.e., H_d at a breast-height age of 50 yr), and $P_{g(jkl)}$ and $T_{g(jkl}$ are respectively, the total precipitation (mm) and the mean temperature (°C) during the growing season specific to the jth geographic locale, kth climate change scenario and lth commitment period (sensu IPCC [10]). Note, $P_{g(jkl)}$ and $T_{g(jkl)}$ values for the jth geographic location as defined by longitude and latitude geographic coordinates, kth climate change scenario as defined by an RCP (IPCC [10]), and lth commitment period (2011–2040, 2041–2070, and 2071–2100), were and are obtainable from the second-generation Canadian Earth System Model (CanESM2; [31]) when used in combination with a spatial-based geo-referencing algorithm [32]. Briefly, the RCPs are differentiated based on the projected change in radiative forcing at the tropopause by 2100 relative to preindustrial levels: e.g., RCP2.6, RCP4.5, and RCP8.5 denote increasingly concerning changes in radiative forcing by 2100 of +2.6, +4.5, and +8.5 watts per square meter (W/m^2), respectively (IPCC [10]). Atmospheric CO_2 levels under the RCP2.6, RCP4.5 and RCP8.5 are expected to increase up to 450 ppm, 550 ppm and 1200 ppm by 2100, respectively (IPCC [10]). The corresponding increase in global mean surface temperature by the end of the 21st century (2081–2100) relative to 1986–2005 is likely to be 0.3–1.7 °C for the RCP2.6, 1.1–2.6 °C for the RCP4.5, and 2.6–4.8 °C for the RCP8.5 (IPCC [10]).

Analytically, given the discontinuous change in height estimates forecasted to occur at the beginning of the commitment periods due to the discrete and dramatic changes in the

estimated climatic input variables, the height estimates were adjusted using a mathematical-based difference method [15]. Furthermore, the cumulative effect of climate change is applied gradually across the years within each commitment period through an annual linear-proportional incremental adjustment to the precipitation and temperature values. This approach yields a continuous mean dominant height - age trajectory for a given climate change scenario and locale. Additionally, deploying the approach previously described for quantifying genetic worth effects on overall stand dynamics [20], a growth modifier that accounts for the age-specific selection gain and its associated temporal correlative decay over the rotation, is also embedded within the site-specific height-age model (i.e., see [20] for full analytical details). Note, although the actual genetic worth effect estimate is specified by the end-user, a meta-based estimate was utilized in this study's exemplification: i.e., an 8% increase in mean dominant height growth at a selection age of 15 years as previously determined for red pine [33]. The remaining five parameterized subordinate modules were then integrated according to the hierarchical structure graphically illustrated in Figure 1, ultimately yielding the red pine SSDMM.

The computation pathways within and between modules as summarized in Figure 1, are also presented in detail in Figure SM2-1. More precisely, as illustrated within these schematic figures, the model requires end-user input in terms of the following crop plan specifics: site index, locale, and a triple-set of density management regimes. As described previously, this specifically includes: (1) establishment density and rotation age; (2) climate change scenario inclusive of associated commitment-period-specific temperature and precipitation values; (3) time, type, growth response model, intensity and costs of thinning treatments when applicable; (4) genetic worth effects, selection age and associated growth response model type when applicable; (5) site preparation, establishment and rotational harvesting costs; and (6) inflation and discount rates, calendar year of simulation, operability targets, merchantability specifications for taper-based stem volume, utility pole, saw log and pulp log calculations, current fiscal worth estimate for standard-sized utility poles, and the preferred operational adjustment factor. Module A then generates regime-specific temporal size–density trajectories in accordance with the (1) specified site quality (site index), establishment density, genetic worth effects, type and intensity of thinning treatments, and density-independent mortality rate (operational adjustment factor), (2) density-dependent mortality sub-model, and (3) locale-specific induced height-growth rate changes specific to the selected climate change scenario. Thinning growth responses, genetic worth effects and climate change effects are all embedded within the biophysical site-based height-age model. Essentially, this computational sequence is consistent with the dynamic SDMD modelling framework in which the resultant temporal dynamical elements of the model, inclusive of anthropogenic effects that together collectively govern stand development patterns and processes, are all embedded within Module A (Figure SM2-1(a)). Module B then links the resultant size–density trajectories and associated stand-level yield metrics produced from Module A to the PPES, enabling the Weibull-based probability density function (PDF) to be recovered at any time point (year) in a plantation's size–density trajectory (i.e., output from Module A is used to populate the PPES; Module B (Figure SM2-1(b)). Furthermore, the resultant composite height-diameter prediction model allows height estimates to be obtained for each recovered diameter class (Module B; Figure SM2-1(b)). Module C then collectively utilizes the output from Module A (quadratic mean diameter estimate) and Module B (diameter and height for each recovered size class) in association with the taper equation, to estimate upper diameter at any stem height position for the median-sized tree within each recovered diameter class (Module C; Figure SM2-1(c)). This enabled the estimation of the potentially extractable log and pole products (i.e., product type, size and associated number for each (pulp logs, saw logs and utility poles)) and residual stem tip volume, at both the diameter class and stand levels. Additionally, via numerical integration, diameter-class-specific estimates of merchantable and total volume were calculated and scaled to the stand level. Module D utilized output from Module B (diameter and height for each diameter class along with the number of trees per class) in conjunction with

the allometric-based component biomass functions, to estimate diameter class and stand level oven-dry biomasses and carbon-mass equivalents, both on a component-specific and collective basis (i.e., periderm, stem, branch, and foliage components and for all components combined) (Module D; Figure SM2-1(d)). Module E and Module F both used output from Module A (mean dominant height and relative density estimates) and Module B (diameter and height for each recovered diameter class along with the number of trees per class) to populate the following relationships: (1) composite sawmill-specific product volume recovery and value functions (Module E; Figure SM2-1(e)); and (2) suite of fibre attribute mixed-effects prediction equations (Module F; Figure SM2-1(f)). This enabled the estimation of the (1) recoverable volumes and associated fiscal worth of sawmill-produced end-products (lumber and chip volumetric yields by sawmill processing protocol (stud and randomized length sawmill configurations)) for each recovered diameter class, and cumulatively at the stand level (Module E; Figure SM2-1(e)), and (2) eight end-product-based fibre determinates (wood density, microfibril angle, modulus of elasticity, fibre coarseness, tracheid wall thickness, tracheid radial diameter, tracheid tangential diameter and specific surface area) for each recovered diameter class from which stand-level mean metrics were derived (Module F; Figure SM2-1(f)). Refer to Figure SM2-1 for an in-depth schematic illustration and corresponding descriptive synthesis of the computational framework within and among all six modules (SM-S2.PDF file; Supplementary Materials).

In summary, the sequential linkage of the six individual modules within a hierarchical-based modelling framework, as illustrated and analytical described in Figure 1 and Figure SM2-1, respectively, yielded the computational pathway utilized within the climate-sensitive red pine SSDMM. Collectively, this pathway enabled the generation of scenario and locale specific rotational estimates of volumetric yields, pole and log product distributions, biomass and carbon sequestration outcomes, sawmill-specific end-product recovery volumes and associated fiscal worth values, wood quality metrics, and ecosystem service performance measures, for any specified crop plan.

3.2. The Red Pine SSDMM-Based Algorithmic Analogue and its Utility

The computational sequence within and among all six modules was subsequently translated and coded into the Fortran programming language, resulting in the red pine crop planning software algorithm. Two model variants were included: (1) climate-insensitive SSDMM which does not explicitly account for climatic effects via the deployment of the non-biophysical version of the site-specific height-age function (Equation (1a)); and (2) climate-sensitive SSDMM which does explicitly account for localized climatic effects through the use of the biophysical version of the site-specific height-age function (Equation (1b)). A number of internal computations and associated validation tests were embedded within the program in order to maintain numeric equivalency among the various yield and end-product related estimates. These included ensuring approximate equivalence between the (1) quadratic mean diameter value generated from the yield–density relationship and that generated from the corresponding recovered diameter distribution (n., recovery of the diameter distribution is negated for a given rotation year if the estimates differ by more than 25%), (2) dominant height estimates derived from the site-specific height-age function and that derived from the recovered height distribution (i.e., rescaling the height distribution to attain equivalence with the site-based dominant height estimate [19]), and (3) merchantable stem volume estimate and the sum of the mill-specific lumber and chip volume estimates (e.g., adjusting the product volume estimates to comply with the merchantable volume estimate when the former is greater than the latter [19]). Additionally, enhanced input options were embedded within the crop planning graphical user interface (GUI) to enable the end-user to introduce or modify various assumptions that could affect volumetric yield and end-product outcomes and related performance indicators. These included the ability to (1) set the operational adjustment factors for density-independent mortality, (2) change merchantability specifications for pole and log products in order to reflect localized harvesting thresholds or market demand requirements, (3) select the type and

growth response rate for genetic worth effects, (4) specify product degrade levels, inflation and discount rates, and (5) apply proprietary-based fixed and variable cost estimates if desired. For the climate-sensitive variant, input for the geo-referenced temperature and precipitation values specific to each commitment period for the selected climate change scenario, is also required (e.g., locale-specific values consistent with a historical normal, RCP4.5 or RCP8.5 scenario).

The computational sequence yields an extensive array of output for each specified crop plan. Specifically, for each rotational year within the predicted size–density trajectory the program recovers the grouped-diameter frequency distribution. For each diameter class recovered, the model provides estimates of the mean total tree height, number of pulp logs, saw logs, and utility poles potentially recoverable, merchantable and total volumes, total and component-specific biomasses and associated carbon mass equivalents, sawmill-specific recoverable chip and lumber volumes and associated fiscal worth values, and mean-tree wood quality attributes. Cumulative total stand-level values are also correspondingly generated. The output is presented in both tabular and graphical formats, inclusive of the size–density trajectories displayed in the traditional SDMD graphic, regime-specific annual estimates at the individual diameter-class level, regime-specific treatment yields and rotational summaries, and regime-based rotational contrasts for a subset of management-relevant performance indicators. The included rotational performance indices were considered key determinates underlying optimal crop plan selection. Specifically, they included the following: (1) overall volumetric, biomass and carbon sequestration productivity as measured by mean annual merchantable volume increment (R_{MAI}; m^3/ha/yr), mean annual biomass increment (R_{BMI}; t/ha) and mean annual carbon increment (R_{CAI}; t/ha), respectively; (2) percentage of saw logs produced (R_{SL}; %); (3) mill-based solid-wood production potential expressed as the percentage of lumber volume recovered via the mth sawmill processing protocol ($R_{LV(m)}$ where $m = s$ (stud mill) or r (randomized length mill); %); (4) number of utility poles produced over the rotation (N_{up}; poles/ha); (5) relative land expectation value specific to the mth sawmill processing protocol ($E_{(m)}$; %); (6) duration of optimal site occupancy (S_O (%); i.e., percentage of the rotation in which the regime was maintained within the optimal relative density management window ($0.35 \leq P_r \leq 0.50$)); (7) stand stability as quantified by the mean height/diameter ratio for the dominant crown classes (S_S; m/m); (8) time to operability status as measured by the number of years that a plantation requires to reach harvestable status as defined by the end-user-specified piece size (number of merchantable stems per cubic metre of merchantable volume) and merchantable yield (merchantable volume per unit area) thresholds (O_T; yr); and (9) suite of Silviscan-based end-product fibre attribute determinates (mean basal-area weighted fibre attribute values for wood density ($\overline{W}_{d(T)}$), microfibial angle ($\overline{M}_{a(T)}$), modulus of elasticity ($\overline{M}_{e(T)}$), fibre-coarseness ($\overline{C}_{o(T)}$), tracheid wall thickness ($\overline{W}_{t(T)}$), tracheid radial diameter ($\overline{D}_{r(T)}$), tracheid tangential diameter ($\overline{D}_{t(T)}$) and specific surface area ($\overline{S}_{a(T)}$)). Refer to Table SM3-1 within the SM-S3.PDF distributed within the Supplementary Materials zip file, for complete computational details underlying these performance indices.

To briefly exemplify the potential utility of the algorithm in crop planning, the output for three conventionally managed plantations which were established on medium-to-good site qualities (i.e., site index of 23 m at a breast-height age of 50 yr [7]) at a single Ontario-centric locale (Thessalon), are presented. Procedurally, the SSDMM software simulations consisted of inputting the required locale-specific bioclimatic variables for an RCP8.5 climate change scenario along with the crop planning details, as presented in Table 1.

Table 1. Input parameters for the SSDMM software simulations for red pine plantations growing on medium-to-good quality sites under a RCP8.5 climate change scenario at Thessalon, Ontario.

Parameter (Units) [a]		Regime 1 (IS)	Regime 2 (IS+1CT)	Regime 3 (IS+2CT)
Rotation age (yr)		75	75	75
Planting year		2022	2022	2022
Simulation years		2022–2097	2022–2097	2022–2097
Initial planting density (stems/ha)		2000	2000	2000
Genetic worth (%)/selection age (yr)		8/15	8/15	8/15
1st CT: stand age (yr)/basal area removal (%)		-	55/35	40/20
2nd CT: stand age (yr)/basal area removal (%)		-	-	55/20
Operational adjustment factor (%)		0.01	0.01	0.01
Climate change variable settings				
Mean temperature during growing season (°C) [*Tg*]	2011–2040	14.49	14.49	14.49
	2041–2070	15.85	15.85	15.85
	2071–2100	17.76	17.76	17.76
Total precipitation during growing season (mm) [*Pg*]	2011–2040	600.0	600.0	600.0
	2041–2070	634.8	634.8	634.8
	2071–2100	620.8	620.8	620.8
Merchantable Specifications				
Pulp log length (m)		2.59	2.59	2.59
Pulp log minimum diameter (inside bark; cm)		10	10	10
Saw log length (m)		5.03	5.03	5.03
Saw log minimum diameter (inside-bark; cm)		14	14	14
Merchantable top diameter (inside-bark cm)		10	10	10
Minimum utility pole length (m)		12.2	12.2	12.2
Minimum pole upper diameter (inside-bark; cm)		19.9	19.9	19.9
Minimum pole diameter class (outside-bark; cm)		34	34	34
Product degrade (%)		10	10	10
Minimum Operability Targets				
Piece-size (merchantable number of stems per cubic metre of merchantable volume)		10	10	10
Merchantable volumetric stand yield (m^3/ha)		200	200	200
Economic Parameters				
Interest rate (%)		2	2	2
Discount rate (%)		4	4	4
Mechanical site preparation (CAN$/ha)		300	300	300
Planting (CAN$/seedling)		0.8	0.8	0.8
Costs of 1st CT: variable (CAN$/$m^3$ of merchantable volume removed)/fixed (CAN$/ha)		-	75/300	75/300
Costs of 2nd CT: variable (CAN$/$m^3$ of merchantable volume removed)/fixed (CAN$/ha)		-	-	65/300
Rotational harvesting+stumpage+renewal+ transportation+manufacturing variable costs (CAN$/$m^3$ of merchantable volume harvested)		75	65	55
Current (2022) net pole value (CAN$K/pole)		0.3	0.3	0.3

Note, all fiscal input variable values are informed approximations. Computationally: (1) variable cost estimates for thinning treatments include all on-site equipment operating costs, stumpage payments, renewal fees, transportation expenses and manufacturing costs and expressed as a function of merchantable volume removed (sensu [34]); (2) fixed cost estimates for thinning included forest management fees (e.g., tree marking) and equipment movement costs (to and from the site); and (3) rotational variable cost estimates for final harvesting include all those associated with harvesting equipment operating, stumpage payments, renewal fees, transportation expenses and manufacturing processing costs and expressed collectively as a function of merchantable volume harvested. [a] A medium-to-good quality site was nominally defined as having a site index value of 23 m (i.e., mean dominant height of 23 m at a breast-height age of 50; [7]). Genetic worth is the percentage increase in dominant height growth expected to occur at the specified selection age (i.e., see [20] for specifics). Operational adjustment factor is the annual mortality rate attributed to non-density-dependent abiotic and biotic causes. Product degrade is an end-user specified allowance for correcting for the potential over-estimation arising from the use of product prediction functions derived from virtual sawmill-based simulations (sensu [35]). All forecasted values for climatic parameters were derived from second generation Canadian Earth System Model (CanESM2; [31]) which consists of a physical atmosphere-ocean model (CanCM4) coupled to a terrestrial carbon model (CTEM) and an ocean carbon model (CMOC). Specific estimates for the Thessalon locale were derived from a customized spatial climatic model [32].

Figure 2 graphically illustrates the predicted temporal mean volume–density trajectories for each crop plan within the traditional SDMD graphic, and Table 2 provides the resultant rotational performance metrics.

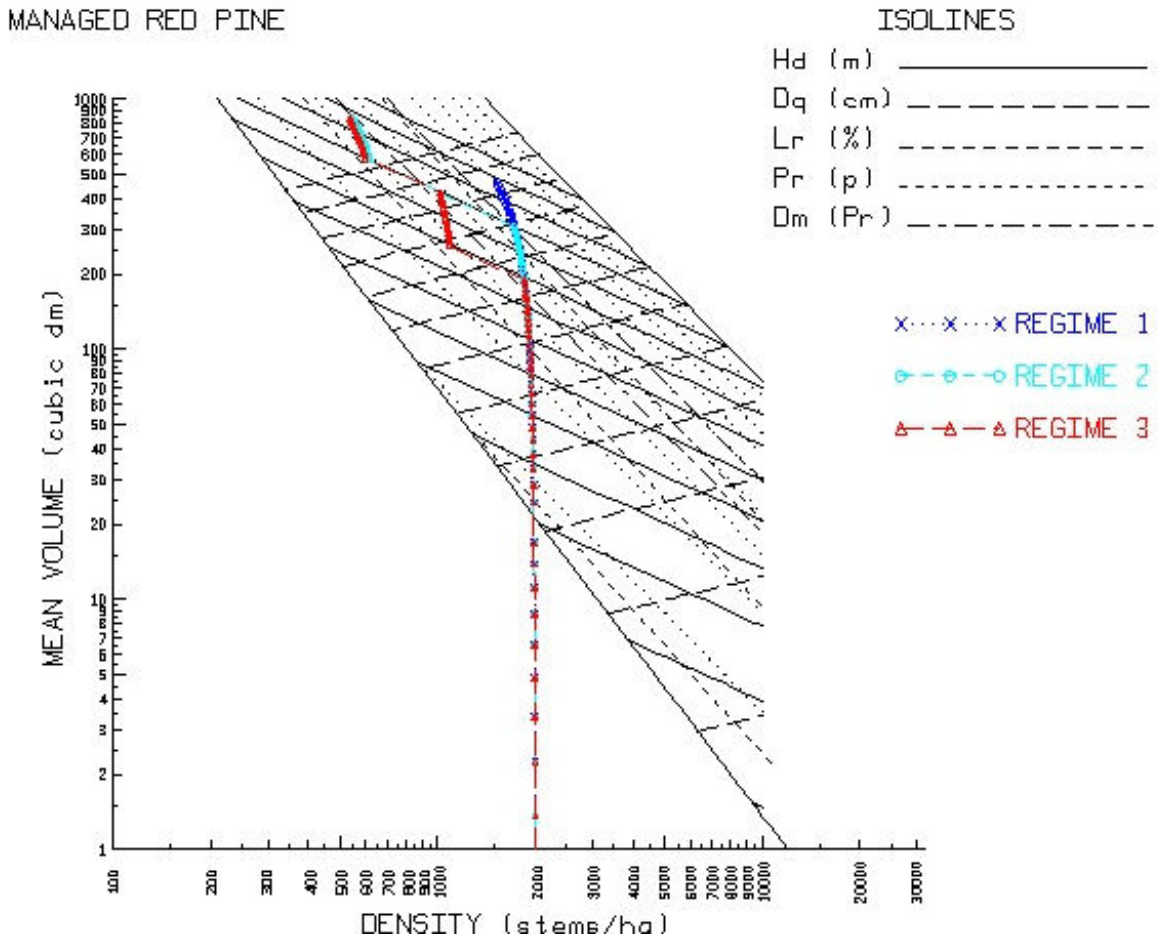

Figure 2. Temporal size–density trajectories for the 3 red pine plantations growing under conditions consistent a RCP8.5 climate change scenario on a medium-to-good site quality (S_I = 23) situated in north-central Ontario (Thessalon) as illustrated within the context of the SDMD graphic. Specifically, graphically illustrating: (1) isolines for mean dominant height (Hd; 4–30 m by 2 m intervals), quadratic mean diameter (Dq; 4–26 cm by 2 cm intervals), mean live crown ratio (Lr; 35, 40, 50, . . . , 80%), relative density index (Pr; 0.1–1.0 by 0.1 intervals); (2) crown closure line (lower diagonal solid line) and self-thinning rule at a Pr = 1.0 (upper diagonal solid line); (3) lower and upper Pr values delineating the optimal density management window (Dm; 0.35 $\leq$ Pr $\leq$ 0.50); and (4) expected 75 year (2022–2097) size–density trajectories with 1 year intervals denoted for each of the specified crop plans. Specifically, Regime 1 representing an initial spacing (2.2 $\times$ 2.2 m)—no-thinning crop plan; Regime 2 representing an initial spacing (2.2 $\times$ 2.2 m) with 1 commercial thinning (CT) treatment (35% basal area removed at 55 yrs) crop plan, Regime 3 representing an initial spacing (2.2 $\times$ 2.2 m) with 2 CT treatments (20% basal area removed at 40 yrs and 55 yrs) crop plan (refer to Table 1 and text for additional crop plan specifics).

Examining these results revealed that relative to the unthinned plantation, the thinned plantations exhibited: (1) moderate declines in merchantable volumetric productivity with the twice-thinned plantation illustrating the highest rate of decline; (2) minor increases in biomass productivity and carbon sequestration potential with the once-thinned plantation exhibiting the largest gain; (3) moderate declines in saw log production with the twice-thinned plantation illustrating a substantially greater rate of reduction; (4) marginal increases in the proportion of recoverable lumber volume irrespective of sawmill processing protocol; (5) consequential increases in economic worth arising from thinning with the twice-thinned plantation exhibiting the largest increase; (6) no change for the single thinned plantation and a major decline for the twice thinned plantation, in the duration of optimal site occupancy; (7) considerable declines in height/diameter ratios and hence

increased stand stability; (8) no change in the time required to attain stand operability status; and (9) although changes were minimal for six of the eight wood quality fibre attributes examined, thinning did elicit substantial increases in microfibial angle and decreases in wood stiffness (modulus of elasticity). Although these specific simulation results and associated inferences suggest that the crop plans which included thinning treatments were less productive in terms of volumetric yield outcomes and produced wood fibre of slightly lower quality in terms of solid wood end-product potential, they did generate consequential increases in mean tree sizes and stand stability, and most importantly enabled the plantations to attained pole production status. The differences between the thinned regimes were marginal for most of these metrics; however, the twice-thinned regime did generate slightly better overall economic worth outcomes.

Table 2. SSDMM-derived rotational stand-level performance indices for 3 crop plans growing under a RCP8.5 for red pine plantations situated in north-central Ontario (Thessalon).

Index [a] (Unit)	Crop Plan [b] Regime 1 IS	Regime 2 IS+1CT	Regime 3 IS+2CT
R_{MAI} (m^3/ha/yr)	9.2	8.4	7.9
R_{BAI} (m^3/ha/yr)	4.9	5.3	5.1
R_{CAI} (m^3/ha/yr)	2.5	2.7	2.6
R_{SL} (%)	56.8	48.4	36.1
$R_{LV(s)}$ (%)	80.8	84.2	84.2
$R_{LV(r)}$ (%)	79.5	81.0	81.3
N_{up} (poles/ha)	0	50	63
$E_{(s)}$ (CAN$k/ha)	11.0	19.6	21.4
$E_{(r)}$ (CAN$k/ha)	7.5	11.2	13.2
S_O (%)	22.7	22.7	12.0
S_S (m/m)	110.6	85.3	90.1
O_T (yr)	30	30	30
$\overline{W}_{d(T)}$ (kg/m^3)	463.5	458.4	458.4
$\overline{M}_{a(T)}$ (°)	12.0	17.1	17.3
$\overline{M}_{e(T)}$ (GPa)	13	10	10
$\overline{C}_{o(T)}$ (µg/m)	488.4	505.7	506.3
$\overline{W}_{t(T)}$ (µm)	3.1	3.0	3.0
$\overline{D}_{r(T)}$ (µm)	32.9	34.2	34.2
$\overline{D}_{t(T)}$ (µm)	30.9	31.7	31.7
$\overline{S}_{a(T)}$ (m^2/kg)	284.5	281.6	281.6

[a] Predicted rotation values; denotations defined within main text; refer to Table SM3-1 for a detailed description of the computations utilized (SM3.PDF file). [b] Crop plan specifics provided in Table 1.

Even though Table 2 provides various management-relevant performance metrics for informing red pine density management decision-making under climate change, the exemplification is very limited in scope (i.e., specific to a single crop plan set, locale, site quality and climate change scenario). Much larger scoped comparisons are required when such models are considered for operational deployment given the uncertainty of climate change severity and its effects on red pine productivity. For example, including multiple climate change scenarios across a larger set of crop plan candidates and geographic locales via extensive iterative-based simulations, would yield a wider perspective on the variability and range of plausible outcomes achievable among crop plans (e.g., [23]). Acknowledging and accommodating such variability will be an essential element to crop planning decision-making during the Anthropocene.

3.3. Analytical Evolution and Expanding Capability of Red Pine SDMD-based Models

Historically, the first SDMD calibrated for red pine was the static variant contributed by Smith and Woods [36]. Although lacking a survivorship sub-model to explicitly ac-

count for density-dependent mortality within the size–density trajectories, the provision of this variant along with a user-friendly software analogue, represented an important step towards the acceptance and deployment of such models in regional stand-level management planning. However, its operational utility eventually became more limited as forest managers increasingly moved towards more complex management goals, such as those involving the realization of end-product production and ecosystem services objectives (sensu [37]). Furthermore, not unlike other stand-level yield prediction models (e.g., benchmark yield curves and the Ontario variant of the Forest Vegetation Simulator [38]), the inability to account for climate change effects on rotational forecasts also became more problematic in terms of the model's operational applicability. Arising from these challenges has been an increasingly important aspirational requirement among red pine managers for an enhanced stand-level decision-support tool. One that could simultaneously forecast rotational outcomes for these diverse objectives while also accounting for climate change effects.

Consequently, the provision of a SSDMM, as presented in this study, that is able to address a multitude of forest management objectives and account for climate change effects on rotational forecasts, represents a tangible first step in accommodating this operational requirement. Additionally, although uniquely relevant to red pine managers, the modelling advancement in terms of enabling the estimation of utility pole production significantly extends the utility of the SSDMM in crop planning. Particularly since utility pole production is considered a defining management performance target among red pine managers given its consequential effect on economic worth outcomes (sensu [39]). Operationally, however, given unknowns with respect to climate mitigation strategies and their effects, a cautionary approach should nevertheless be exercised when explicitly interpreting model predictions and associated crop planning inferences, particularly those pertaining to the later commitment periods. Given that progress toward climate-sensitive spatial-specific crop planning with respect to Canadian conifers has been challenging given the paucity of applicable stand-level decision-support tools, the introduction of the red pine SSDMM represents an incremental step towards spatial-explicit crop planning under climate change. Demonstrating such utility along with an assessment of the model's predictive ability is the focus of ongoing research efforts and will be reported on separately (i.e., [23]).

Analytically, SSDMMs evolved from the approach used to develop dynamic stand density management diagrams (sensu [40,41]), which were themselves derived from the foundational static SDMD that was initially advanced by Ando [42]. Briefly, the static, dynamic and structural model variants share commonalities in terms of their underlying qualitative ecological foundation and associated quantitative representations, which when integrated comprise their core analytical structure (e.g., see [14,26,43] for comprehensive summaries). More precisely, the static diagrams introduced by Ando [42,44] in Japan and Drew and Flewelling [43,45] in New Zealand and the Pacific Northwest, the dynamic diagrams proposed by Newton and Weetman [40,41] in Canada and Stankova and Shibuya [46] in Europe, and the structural diagrams presented by Newton [17–19,47,48] in Canada and by Stankova and Diéguez-Aranda [49] in Europe, all share commonalities with respect to resource competition axioms, self-thinning theory, reciprocal yield–density relationships, site occupancy—forest productivity constructs (e.g., [50–52]) and stand dynamical determinates (e.g., site quality effects on stand developmental rates and self-thinning processes). The resultant quantitative analogues of these qualitative commonalities are key analytical pillars of all three model variants. These include the (1) -3/2 self-thinning rule [53], (2) reciprocal equations of the competition–density and yield–density effect [54–56] or their empirical equivalents (e.g., [43]), (3) volume-based relative density indices and associated thresholds delineating the (i) likelihood of imminent competition–mortality occurring [45], and (ii) optimal productivity zones based on Langsaeter's [50] site occupancy—productivity relationship (e.g., [40,57]), and (4) size–density relationship defining the beginning-curve of competition [42] also known as the crown closure line [45].

Collectively, the overwhelming empirical evidence in support of the applicability of these underlying ecological axioms and associated functional relationships across multiple stand-types throughout the temperate and boreal forest biomes (e.g., [58]), bodes well for the continued development and deployment of SDMD-based models in crop planning decision-making. Furthermore, their ecological foundation and associated allometric structure allow these models to be readily modified and adapted for ongoing consequential changes in overall growing conditions (e.g., climate change), tree improvement (e.g., genetic worth effects), management objectives and perspectives (e.g., carbon sequestration and conservation), and market requirements (e.g., utility poles), as demonstrated in this study. Overall, the climate-sensitive red pine SSDMM not only increments the analytical SDMD-based modelling legacy established over the last 60 years but also has the potential to facilitate the paradigm shift towards spatial-based climate-smart crop planning and silvicultural decision-making.

4. Conclusions

Red pine is an intensely managed species throughout the southern boreal and northern temperate forest regions of central North America. Although the species responds readily to stand density management treatments as extensively documented in the forestry literature, the lack of stand-level decision-support models that can account for localized climate change effects and provide quantitative insights into their potential consequences in terms of volumetric yield, end-product diversity and ecosystem service outcomes, has hindered crop planning. Consequently, this study developed a climate-sensitive modular-based SSDMM for red pine in order to address this shortcoming. The presented model incrementally contributes to the growing portfolio of structural stand density management decision-support systems developed for managing commercially important coniferous species. The analytical approach that was utilized preserved the advantageous qualitative concepts (e.g., self-thinning, yield-density and forest production axioms) and quantitative elements (e.g., functional solutions for both density-independent and density-dependent mortality processes and accounting for thinning and genetic worth effects on temporal stand-dynamics) of the previous static, dynamic, and structural modelling platforms. Furthermore, the effects of climate change on stand dynamical processes were explicitly accounted for via the deployment of a biophysical site productivity function (e.g., inclusion of rate parameter modifiers (precipitation and temperature) within the principal functional determinate governing temporal stand development (site-based height-age equation)). The resultant red pine SSDMM and associated algorithmic analogue enabled the evaluation of crop planning efficiency across a wide array of forest management perspectives while also accounting for localized climate change effects. Additionally, expanding the scope of the SSDMM structure via the addition of a new product class (utility pole production), yielded a much-needed crop planning outcome metric given the importance of this commodity within the red pine forest products supply chain. In summary, the model's novel ability to forecast rotational outcomes inclusive of utility pole production and evaluate competing crop plan efficiencies across a multitude of forest management perspectives and climate change scenarios, should be of consequential utility as the complexities of red pine crop planning intensify during the Anthropocene.

Funding: This research was funded by the Canadian Wood Fibre Centre, Canadian Forest Service, Natural Resources Canada.

Supplementary Materials: The following is available online at https://www.mdpi.com/article/10.3390/f13071010/s1. This file includes 3 pdf files: (1) SM-S1.PDF file consisting of the analytical description of the development of the modular structural stand density management model (SSDMM) for red pine, and is entitled "Modular-specific Development of the Red Pine Structural Stand Density Management Model"; (2) SM-S2.PDF file consisting of comprehensive schematic illustrations and numerical descriptions of the computational framework utilized within the modular-based SSDMM for red pine, and is entitled "SSDMM Computational Sequence"; and (3) SM-S3.PDF file consisting of

computational analytics underlying the stand-level performance indices, and is entitled "Performance Indices: computations and denotations".

Institutional Review Board Statement: Not applicable.

Informed Consent Statement: Not applicable.

Data Availability Statement: Not applicable.

Acknowledgments: The author expresses his appreciation to (1) Scott McPherson, previously with the Ontario Ministry of Natural Resources (Southern Science and Information Unit, North Bay, Ontario, Canada) for providing the majority of the calibration data sets utilized, and (2) journal reviewers and editors for their constructive comments and suggestions.

Conflicts of Interest: The author declares no conflict of interest.

Appendix A

Table A1. Mensurational summary of the calibration data set: plot, treatment, site quality and stand attributes by sample cluster.

Cluster	No. Plots	No. Meas.	Number of Thinnings								Plot Size (ha)	Stand Age (yr)			Dominant Height (m)			Site Index [a]		
			0	1	2	3	4	5	6	7		Mean	Min	Max	Mean	Min	Max	Mean	Min	Max
AECL	10	7-8	x								0.101	28	10	45	14.6	4.1	24.2	20.0	18.1	21.2
Ballycroy	4	4	x			x	x				0.040	29	21	39	27.1	25.5	28.4	27.2	27.1	27.4
Barr North	2	4		x							0.138	47	34	58	31.1	30.3	31.7	23.5	23.5	23.5
Charlebois	8	5	x			x	x				0.040	45	29	60	27.1	23.8	30.4	23.0	22.1	23.9
Durham UX Main	2	4			x						0.081	59	51	69	29.9	29.3	30.4	21.0	20.9	21.0
Durham UX West	2	4		x							0.081	58	50	68	30.1	29.5	30.7	21.4	21.2	21.5
Flinton	1	3				x					0.081	51	46	57	29.2	28.7	30.0	22.3	22.3	22.3
Kirkwood	4	9	x			x					0.202	58	34	87	29.1	26.4	33.3	21.5	20.8	22.0
Larose	5	4	x		x						0.040	35	24	45	27.4	24.1	29.7	26.5	26.0	26.8
Limerick South	4	7			x	x					0.040	39	28	55	27.4	25.1	30.1	25.0	24.5	25.3
McArthur	2	4	x								0.081	36	28	46	28.0	26.5	29.4	26.1	26.1	26.1
Orr Lake Hamilton	4	9	x			x	x			x	0.101	46	31	65	29.1	26.5	31.0	23.8	23.4	24.1
Orr Lake Main	3	7				x	x				0.040	53	34	73	28.9	26.6	30.9	22.1	21.8	22.3
Orr Lake Stoney	6	8	x		x						0.040	49	35	66	28.7	26.9	30.5	22.8	22.6	22.9
Orrock North East	11	6-8	x	x	x	x					0.040	44	29	71	27.8	24.4	30.8	23.6	22.9	24.4
Orrock South	4	8				x					0.040	43	29	60	29.0	26.8	30.8	24.8	24.6	25.0
Rockland	2	10	x				x				0.202	52	27	75	21.3	12.8	27.4	17.0	16.1	18.1
Sauble Beach	11	3-5		x	x						0.040	42	31	53	26.7	24.2	29.4	23.3	22.6	24.8
Slessor	2	6	x	x							0.081	38	22	54	28.5	26.5	30.0	25.3	25.2	25.4
Thunder Bay	3	4	x								0.130	40	32	47	17.2	14.1	20.1	17.0	15.8	18.0
Vivian	8	9	x				x				0.101	54	38	73	28.9	24.8	31.1	21.7	20.6	22.6

Cluster	D_q (cm)			G (m^2/ha)			V_t (m^3/ha)				V_m (m^3/ha)			N (stems/ha)		
	Mean	Min	Max	Mean	Min	Max	Mean	Min	Max	Mean	Min	Max	Mean	Min	Max
AECL	17.0	4.8	35.0	39.8	1.1	67.6	327.6	2.4	781.3	316.7	0.2	770.0	1913	509	4071
Ballycroy	17.7	14.9	20.2	34.6	25.2	42.7	378.5	268.7	482.0	339.9	237.0	440.7	1417	975	1775
Barr North	34.2	29.5	38.5	66.9	49.5	92.8	865.2	651.7	1206.0	821.8	620.8	1146.4	747	425	971
Charlebois	19.1	13.4	28.1	53.3	29.2	72.8	583.6	345.0	801.4	522.1	308.0	742.4	2247	600	4925
Durham UX Main	27.1	24.3	29.5	68.2	57.6	85.4	841.9	718.2	1033.6	792.6	677.6	968.6	1210	938	1778
Durham UX West	27.7	25.3	30.2	69.6	61.9	81.3	865.3	760.4	1030.3	816.0	715.3	975.1	1156	1037	1247
Flinton	25.2	22.9	28.1	57.1	54.4	59.3	692.3	657.4	716.9	649.1	616.0	676.6	1169	926	1444
Kirkwood	23.9	16.8	33.4	45.1	14.5	66.5	533.7	193.0	766.5	496.5	180.1	711.9	1116	342	2302
Larose	19.1	13.0	26.0	72.2	41.7	106.1	812.4	410.5	1272.5	734.0	333.2	1194.3	2720	1600	4700
Limerick South	19.4	14.3	27.4	75.8	52.6	103.8	843.2	611.7	1113.9	760.6	565.2	1004.3	2944	900	5100

Table A1. *Cont.*

Cluster	No. Plots	No. Meas.	Number of Thinnings							Plot Size (ha)	Stand Age (yr)			Dominant Height (m)			Site Index [a]		
			0	1	2	3	4	5	6	7		Mean	Min	Max	Mean	Min	Max	Mean	Min	Max
McArthur	18.7	15.3		22.0			17.0		12.1		24.4	191.7	126.8	287.7	173.8	109.2	266.9	623	420	864
Orr Lake Hamilton	23.3	16.5		31.8			74.9		48.0		107.5	884.3	608.2	1266.4	821.0	574.9	1176.5	1932	653	4079
Orr Lake Main	22.7	17.0		30.4			75.4		34.6		97.0	878.6	437.5	1124.2	811.2	413.8	1038.2	2155	500	3850
Orr Lake Stoney	21.9	17.0		28.0			77.3		53.3		112.3	900.0	618.4	1273.8	830.8	572.3	1166.8	2227	1000	4200
Orrock North East	20.4	14.5		31.4			67.1		33.0		111.0	763.2	359.9	1213.3	697.0	308.0	1139.8	2269	500	5600
Orrock South	23.9	17.1		32.4			71.6		57.6		83.4	850.5	739.0	1041.4	791.0	700.4	982.6	1780	700	3425
Rockland	27.8	15.6		51.3			55.8		32.2		78.5	501.9	187.6	757.9	396.7	130.2	631.1	1218	380	2412
Sauble Beach	17.5	13.5		26.8			74.9		16.9		107.2	803.9	207.7	1167.1	710.6	195.6	1034.9	3499	300	5300
Slessor	22.4	17.8		26.9			58.3		34.6		88.9	686.0	380.2	1079.4	636.9	344.3	1011.8	1519	802	2321
Thunder Bay	23.9	17.2		31.0			61.2		42.6		81.5	473.1	331.6	612.0	399.5	294.8	494.0	1608	761	2826
Vivian	24.1	14.8		34.8			67.8		34.1		89.5	809.7	405.5	1103.9	754.6	378.1	1046.7	1612	733	3723

Denotations: (1) Number of periodic remeasurements per plot within a given cluster (No. Meas.); (2) Min and Max refer to minimum and maximum values respectively; (3) D_q, G, V_t, V_m and N refer quadratic mean diameter, basal area, total volume, merchantable volume and stand density, respectively (see Section 2.1 for computational specifics). [a] Mean dominant height at a breast-height age of 50 yr [7].

References

1. Rowe, J.S. *Forest Regions of Canada*; Publication No. 1300; Government of Canada, Department of Environment, Canadian Forestry Service: Ottawa, ON, Canada, 1972.
2. Wilson, T.S.; Ryan, C.L. Northern Lakes and Forests Ecoregion. In *Status and Trends of Land Change in the Midwest-South Central United States—1973 to 2000*; Auch, R.F., Karstenson, K.A., Eds.; U.S. Geological Survey Professional Paper 1794-C; U.S. Geological Survey: Sioux Falls, SD, USA, 2015. Available online: https://pubs.usgs.gov/pp/1794/c/pp1794c.pdf (accessed on 2 February 2022).
3. Homagin, K.; Shahi, C.K.; Carmean, W.H.; Leitch, M.; Bowling, C. Growth and yield comparisons for red pine, white spruce and black spruce plantations in northwestern Ontario. *For. Chron.* **2011**, *87*, 494–503. [CrossRef]
4. Flannigan, M.D.; Woodward, F.I. Red pine abundance: Current climatic control and responses to future warming. *Can. J. For. Res.* **1994**, *24*, 1166–1175. [CrossRef]
5. Fei, S.; Desprez, J.M.; Potter, K.M.; Jo, I.; Knott, J.A.; Oswalt, C.M. Divergence of species responses to climate change. *Sci. Adv.* **2017**, *3*, e1603055. [CrossRef] [PubMed]
6. Ashiq, M.W.; Anand, M. Spatial and temporal variability in dendroclimatic growth response of red pine (Pinus resinosa Ait.) to climate in northern Ontario, Canada. *For. Ecol. Manag.* **2016**, *372*, 109–119. [CrossRef]
7. Sharma, M.; Parton, J. Climatic effects on site productivity of red pine plantations. *For. Sci.* **2018**, *64*, 544–554. [CrossRef]
8. Magruder, M.; Chhin, S.; Palik, B.; Bradford, J.B. Thinning increases climatic resilience of red pine. *Can. J. For. Res.* **2013**, *43*, 878–889. [CrossRef]
9. Nabuurs, G.-J.; Mrabet, R.; Abu Hatab, A.; Bustamante, M.; Clark, H.; Havlík, P.; House, J.; Mbow, C.; Ninan, K.N.; Popp, A.; et al. Agriculture, Forestry and Other Land Uses (AFOLU). In *IPCC, 2022: Climate Change 2022: Mitigation of Climate Change. Contribution of Working Group III to the Sixth Assessment Report of the Intergovernmental Panel on Climate Change*; Shukla, P.R., Skea, J., Slade, R., Al Khourdajie, A., van Diemen, R., McCollum, D., Pathak, M., Some, S., Vyas, P., Fradera, R., et al., Eds.; Cambridge University Press: Cambridge, UK; New York, NY, USA, 2022.
10. Intergovernmental Panel on Climate Change (IPCC). *Climate Change 2014: Synthesis Report. Contribution of Working Groups I, II and III to the Fifth Assessment Report of the Intergovernmental Panel on Climate Change*; Core Writing Team, Pachauri, R.K., Meyer, L.A., Eds.; IPCC: Geneva, Switzerland, 2014; p. 151. [CrossRef]
11. MacDonald, H.; McKenney, D.W.; Pedlar, J.H.; Hope, E.; McLaven, K.; Perry, S. Adoption influences in Ontario's 50 million tree program. *For. Chron.* **2018**, *94*, 221–229. [CrossRef]
12. Penner, M.; Pitt, D. The Ontario Growth and Yield Program Status and Needs—Report to the Forestry Futures Trust Committee. 2019. Available online: http://www.forestryfutures.ca/upload/464883/documents/3D5D439A749A7C88.pdf (accessed on 4 February 2022).
13. Porté, A.; Barlelink, H.H. Modelling mixed forest growth: A review of models for forest management. *Ecol. Mod.* **2002**, *150*, 141–188. [CrossRef]
14. Newton, P.F. Stand density management diagrams: Modelling approaches, variants and exemplification of their potential utility in crop planning. *Can. J. For. Res.* **2021**, *51*, 236–256. [CrossRef]
15. Newton, P.F. Simulating the potential effects of a changing climate on black spruce and jack pine plantation productivity by site quality and locale through model adaptation. *Forests* **2016**, *7*, 223. [CrossRef]
16. McIntosh, B.S.; Ascough II, J.C.; Twerym, M.; Chew, J.; Elmahdi, A.; Haase, D.; Harou, J.J.; Hepting, D.; Cuddy, S.; Jakeman, A.J.; et al. Environmental decision-support systems (EDSS) development—Challenges and best practices. *Environ. Model. Softw.* **2011**, *26*, 1389–1402. [CrossRef]
17. Newton, P.F. Croplanner: A stand density management decision-support software suite for addressing volumetric yield, end-product and ecosystem service objectives when managing boreal conifers. *Forests* **2021**, *12*, 448. [CrossRef]
18. Newton, P.F. Development of an integrated decision-support model for density management within jack pine stand-types. *Ecol. Model.* **2009**, *220*, 3301–3324. [CrossRef]
19. Newton, P.F. A decision-support system for density management within upland black spruce stand-types. *Environ. Model. Softw.* **2012**, *35*, 171–187. [CrossRef]
20. Newton, P.F. Genetic worth effect models for boreal conifers and their utility when integrated into density management decision-support systems. *Open J. For.* **2015**, *5*, 105–115. [CrossRef]
21. Newton, P.F. Quantifying growth responses of black spruce and jack pine to thinning within the context of density management decision-support systems. *Open J. For.* **2015**, *5*, 409–421. [CrossRef]
22. Newton, P.F. Wood quality attribute models and their utility when integrated into density management decision-support systems for boreal conifers. *For. Ecol. Manag.* **2019**, *438*, 267–284. [CrossRef]
23. Newton, P.F. Potential Utility of a Climate-sensitive Structural Stand Density Management Model for Red Pine Crop Planning. **2022**. *in preparation*.
24. Peng, C.; Zhang, L.; Liu, J. Developing and validating nonlinear height-diameter models for major tree species of Ontario's boreal forests. *North. J. Appl. For.* **2001**, *18*, 87–94. [CrossRef]

25. Honer, T.G.; Ker, M.F.; Alemdag, I.S. *Metric Timber Tables for the Commercial Tree Species of Central and Eastern Canada*; Information Report M-X-140; Government of Canada, Department of Agriculture, Canadian Forestry Service, Maritimes Forest Research Centre: Fredericton, NB, Canada, 1983.
26. Newton, P.F. Stand density management diagrams: Review of their development and utility in stand-level management planning. *For. Ecol. Manag.* **1997**, *98*, 251–265. [CrossRef]
27. Sharma, M. Incorporating stand density effects in modeling the taper of red pine plantations. *Can. J. For. Res.* **2020**, *50*, 751–759. [CrossRef]
28. Lambert, M.-C.; Ung, C.-H.; Raulier, F. Canadian national tree aboveground biomass equations. *Can. J. For. Res.* **2005**, *35*, 1996–2018. [CrossRef]
29. Newton, P.F. Species-specific whole-stem equation suites for predicting end-product-based wood attribute determinates for jack pine and red pine and their potential utility in crop planning. **2022**. *in preparation*.
30. Weiskittel, A.R.; Hann, D.W.; Kershaw, J.A., Jr.; Vanclay, J.K. *Forest Growth and Yield Modeling*; Wiley-Blackwell: Hoboken, NJ, USA, 2011. [CrossRef]
31. Environment and Climate Change Canada. Second Generation Canadian Earth System Model [online]. 2020. Available online: https://www.ec.gc.ca/ccmac-ccma/default.asp?lang=En&n=1A3B7DF1-1&wbdisable=true (accessed on 4 June 2020).
32. McKenney, D.; Hutchinson, M.F.; Papadopol, P.; Lawrence, K.; Pedlar, J.; Campbell, K.; Milewska, E.; Hopkinson, R.F.; Price, D.; Owen, T. Customized spatial climate models for North America. *Bull. Am. Meteorol. Soc.* **2011**, *92*, 1611–1622. [CrossRef]
33. Newton, P.F. Systematic review of yield responses of four North American conifers to forest tree improvement practices. *For. Ecol. Manag.* **2003**, *172*, 29–51. [CrossRef]
34. Tong, Q.J.; Zhang, S.Y.; Thompson, M. Evaluation of growth response, stand value and financial return for pre-commercially thinned jack pine stands in Northwestern Ontario. *For. Ecol. Manag.* **2005**, *209*, 225–235. [CrossRef]
35. Tong, Q.J.; Zhang, S.Y. Development of lumber recovery correction models for plantation-grown Pinus banksiana trees. *Scand. J. For. Res.* **2009**, *24*, 417–424. [CrossRef]
36. Smith, D.J.; Woods, M.E. *Red Pine and White Pine Density Management Diagrams for Ontario*; Technical Report No. 48; Ontario Ministry of Natural Resources Southcentral Sciences Section: North Bay, ON, Canada, 1997.
37. Nilsson, S. Transition of the Canadian forest sector. In *The Future Use of Nordic Forests-A Global Perspective*; Westholm, E., Lindahl, K.B., Kraxner, F., Eds.; Springer: Cham, Switzerland, 2015; pp. 125–144. [CrossRef]
38. Sharma, M.; Parton, J.; Woods, M.; Newton, P.; Penner, M.; Wang, J.; Stinson, A.; Bell, F.W. Ontario's forest growth and yield modelling program: Advances resulting from the Forestry Research Partnership. *For. Chron.* **2008**, *84*, 694–703. [CrossRef]
39. Grossman, G.H.; Potter-Witter, K. Economics of red pine management for utility pole timber. *NJAF* **1991**, *8*, 22–25. [CrossRef]
40. Newton, P.F.; Weetman, G.F. Stand density management diagrams and their utility in black spruce management. *For. Chron.* **1993**, *69*, 421–430. [CrossRef]
41. Newton, P.F.; Weetman, G.F. Stand density management diagram for managed black spruce stands. *For. Chron.* **1994**, *70*, 65–74. [CrossRef]
42. Ando, T. *Growth Analysis on the Natural Stands of Japanese red Pine (*Pinus densiflora *Sieb. et. Zucc.). II. Analysis of Stand Density and Growth*; Bulletin of the Government Forest Experiment Station No. 147; Government of Japan: Tokyo, Japan, 1962; (In Japanese; English Summary).
43. Drew, T.J.; Flewelling, J.W. Stand density management: An alternative approach and its application to Douglas-fir plantations. *For. Sci.* **1979**, *25*, 518–532.
44. Ando, T. *Ecological Studies on the Stand Density Control in Even-Aged Pure Stands*; Bulletin of the Government Forest Experiment Station No. 210; Government of Japan: Tokyo, Japan, 1968; (In Japanese; English Summary).
45. Drew, T.J.; Flewelling, J.W. Some recent Japanese theories of yield-density relationships and their application to Monterey pine plantations. *For. Sci.* **1977**, *23*, 517–534.
46. Stankova, T.V.; Shibuya, M. Stand density control diagrams for Scots pine and Austrian black pine plantations in Bulgaria. *New For.* **2007**, *34*, 123–141. [CrossRef]
47. Newton, P.F. Development and utility of an ecological-based decision-support system for managing mixed coniferous forest stands for multiple objectives. In *Ecological Modeling*; Zhang, W., Ed.; Environmental Science, Engineering and Technology Book Series; Nova Scientific Publishers: Hauppauge, NY, USA, 2012; pp. 115–172. ISBN 978-1-61324-567-5.
48. Newton, P.F. A silvicultural decision-support algorithm for density regulation within peatland black spruce stands. *Comput. Electron. Agric.* **2012**, *80*, 115–125. [CrossRef]
49. Stankova, T.V.; Diéguez-Aranda, U. Dynamic structural stand density management diagrams for even-aged natural stands and plantations. *For. Ecol. Manag.* **2020**, *458*, 117733. [CrossRef]
50. Langsaeter, A. Om tynning i enaldret gran- og furuskog (About thinning in even-aged stands of spruce, fir and pine). *Meddel. F. D. Norske Skogforsoksvesen* **1941**, *8*, 131–216.
51. Mar:Möller, C.M. The influence of thinning on volume increment. I. Results of investigations. In *Thinning Problems and Practices in Demark*; Technical Publication, 76.; Möller, C., Abell, J., Jagd, T., Juncker, F., Eds.; State University of New York, College of Forestry: Syracuse, NY, USA, 1954; pp. 5–32.
52. Assmann, E. *The Principles of Forest Yield Study*, 1st ed.; Pergamon Press Ltd.: Oxford, UK, 1970. [CrossRef]

53. Yoda, K.; Kira, T.; Ogawa, H.; Hozumi, K. Self-thinning in overcrowded pure stands under cultivated and natural conditions. *J. Biol. (Osaka City Univ. Jpn.)* **1963**, *14*, 107–129.
54. Kira, T.; Ogawa, H.; Sakazaki, N. Intraspecific competition among higher plants. I. Competition-yield-density interrelationship in regularly dispersed populations. *J. Inst. Poly. Osaka City Univ. D* **1953**, *4*, 1–16.
55. Shinozaki, K.; Kira, T. Intraspecific competition among higher plants. *VII. Logistic theory of the C-D effect. J. Inst. Polytech. Osaka City Univ. Ser.* **1956**, *7*, 35–72.
56. Shinozaki, K.; Kira, T. Intraspecific competition among higher plants. X. The C-D rule, its theory and practical uses. *J. Biol. Osaka City Univ.* **1961**, *12*, 69–82.
57. Newton, P.F. Forest production model for upland black spruce stands-optimal site occupancy levels for maximizing net production. *Ecol. Model.* **2006**, *190*, 190–204. [CrossRef]
58. Newton, P.F. Evaluating the ecological integrity of structural stand density management models developed for boreal conifers. *Forests* **2015**, *6*, 992–1030. [CrossRef]